

Dislocation drag in sodium chloride at low temperature—A radiation-damping model*

A. Hikata and C. Elbaum

Brown University, Providence, Rhode Island 02912

(Received 7 January 1974)

The contribution of dislocations to ultrasonic attenuation in the liquid-helium temperature range has been measured in sodium chloride for the purpose of determining the resistive force acting on dislocations. Use was made of a technique for measuring the ultrasonic attenuation change $\Delta\alpha$ at different frequencies, caused by a bias stress. The predictions of the extensible-string model of dislocations, which account well for the behavior of $\Delta\alpha$ above about 70 °K, are not consistent with the observed frequency and amplitude dependence of $\Delta\alpha$ at lower temperatures. A dislocation-drag model based on a radiation-damping mechanism is shown to account for the present results. Furthermore, this mechanism, taken in conjunction with the viscous damping normally assumed for the extensible-string model, also accounts qualitatively for the behavior of dislocation damping at low frequencies (kHz), which shows discrepancies with the string model.

I. INTRODUCTION

When a dislocation in a crystal is set in motion, it experiences a resistive force leading to energy dissipation. There are several physical mechanisms giving rise to these resistive forces, i. e., it is possible to have different energy dissipation processes for a moving dislocation. In general, the sources of the resistive force (drag) may be classified into two categories, "intrinsic" and "extrinsic." The extrinsic sources are obstructive barriers against dislocation motion, such as impurities, precipitates, other dislocations, grain boundaries, etc., where a moving dislocation may be held up for a certain period of time in course of its motion. The dislocation may overcome the barriers with the help of thermal fluctuations. Therefore, the average dislocation velocity is influenced greatly by the waiting time spent at the barriers. In particular, the drag determined by methods which involve large displacements of individual dislocations (produced for example by stress pulses of known magnitude and duration)¹ may be strongly influenced by these extrinsic sources. Dislocation drag determined from ultrasonic attenuation studies, on the other hand, provides a measure of the intrinsic resistive force. This is because the dislocation displacements (oscillatory) caused by ultrasonic waves are small, so that the interactions between dislocations and the extrinsic barriers are very infrequent and can be neglected.

The intrinsic resistive force originates from the intrinsic properties of the crystal, which may be subdivided into two categories, (i) elementary excitations (e. g., phonons and conduction electrons), and (ii) discreteness of crystal lattice structure. Phonons and, in the case of metals, conduction electrons interact with dislocations through the process of scattering, and produce resistive forces upon moving dislocations. Theoretical treatments

of this subject are given by several investigators,²⁻⁴ and they all agree in that the drag force F caused by such mechanisms is proportional to the dislocation velocity v (viscous type damping):

$$F = Bv .$$

The proportionality constant B is called (viscous) damping constant or drag coefficient. It should be emphasized here, however, that in the scattering theories so far presented, dislocation configurations are treated within the framework of continuum theory of elasticity, and the discreteness of lattice structure is not taken into account. We have investigated experimentally the values of B and its temperature dependence for lead,⁵ aluminum⁶ and sodium chloride,⁷ and obtained reasonable agreement with the predictions of the scattering theories, except that in the case of sodium chloride the experimental results obtained in the temperature range 2–70 °K were found to be inconsistent with the predictions of viscous-type damping. We therefore concentrated our attention on the other intrinsic source of dissipation; namely, the discreteness of lattice structure. It is this point that we treat here in some detail.

II. EXPERIMENTAL TECHNIQUE

The experiments consist of measuring concurrently changes in attenuation $\Delta\alpha$ and modulus defect [in terms of velocity change $\Delta(\Delta V/V)$] caused by an applied dynamic bias stress. The dynamic bias stress method, which is described in previous publications,^{6,7} is a way of extracting the dislocation contributions from the total ultrasonic attenuation by applying a second ultrasonic wave (low frequency and high amplitude) in a direction perpendicular to that of the attenuation-measuring wave. The change $\Delta\alpha$ in attenuation and $\Delta(\Delta V/V)$ in velocity caused by the bias stress wave is measured as a function of frequency ν at a given temperature.

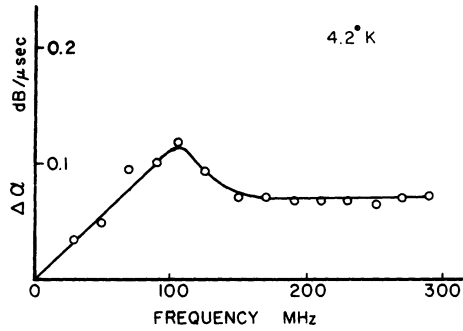


FIG. 1. Attenuation change $\Delta\alpha$ caused by a dynamic bias stress vs frequency, $T=4.2^\circ\text{K}$.

These $\Delta\alpha - \nu$ and $\Delta(\Delta V/V) - \nu$ relations are the subject of analysis in terms of various models. In this study, however, an additional precaution had to be taken concerning the amplitude of the measuring wave. As will be discussed later, the attenuation change $\Delta\alpha$ is found to be sensitive to the amplitude of the measuring wave. It is therefore essential to keep this amplitude constant for every frequency at which the measurements are taken. To this end, a voltage pickup consisting of 40:1 resistive voltage divider is installed right at the transducer, which enables one to monitor the voltage applied to the transducer at each frequency.

The changes in velocity $\Delta(\Delta V/V)$ were determined by means of an interferometric technique, which is a modified version of a method described by Blume.⁸ Particular attention was directed to eliminating spurious indications of velocity changes associated with changes in echo amplitude. Details of this technique will be published separately.⁹

The samples used are single crystals of sodium chloride cleaved from optical grade ingots supplied by the Harshaw Chemical Company. The size of the samples is approximately $7 \times 7 \times 8$ mm, and the faces are perpendicular to $\langle 100 \rangle$ crystallographic directions. After cleaving, two sets of faces of the sample are ground slightly to obtain flat and paral-

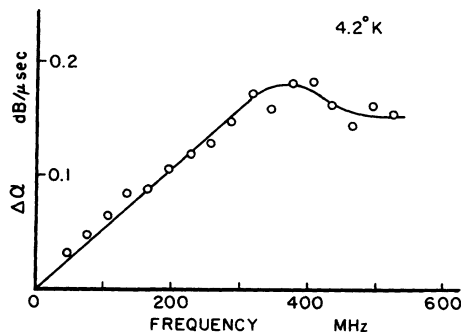


FIG. 2. Same as Fig. 1 for a different sample.

lel surfaces for the purpose of ultrasonic wave propagation.

For the measuring wave, 10 or 15 MHz transducers (either quartz or LiNbO_3) are used at the odd harmonics of their fundamental frequency. For the bias stress wave, 5 or 10 MHz transducers [quartz or lead zirconate (PZT5)] are used at their fundamental frequency. As a bonding agent for the transducers, 1-pentene is used. Since pentene is highly volatile at room temperature, bonds were made at temperatures slightly above its freezing temperature.

III. RESULTS AND DISCUSSION

A. General background

Examples of the $\Delta\alpha$ as a function of frequency ν obtained at 4.2°K for three different samples are shown in Figs. 1–3. Here in contrast to the behavior of the $\Delta\alpha - \nu$ relation above 70°K ,⁷ $\Delta\alpha$ increases with frequency essentially linearly up to a frequency in excess of 100 MHz (the exact value of this frequency varies from sample to sample), then levels off and becomes independent of frequency; in about half the cases a “hump” appears prior to $\Delta\alpha$ leveling off, as seen in Figs. 1 and 2.

As mentioned in Ref. 7, we concluded that at low temperatures (below 70°K) contributions from mechanisms other than viscous damping become important. The main reasons leading to this conclusion are as follows: First, if the drag coefficient B is proportional to the thermal energy density ϵ , which is the approach taken in Ref. 7, and since ϵ decreases with temperature quite rapidly below 70°K , the incremental attenuation $\Delta\alpha$ for a given magnitude of the bias stress also should decrease rapidly with decreasing temperature. Experimentally observed magnitudes of $\Delta\alpha$, however,

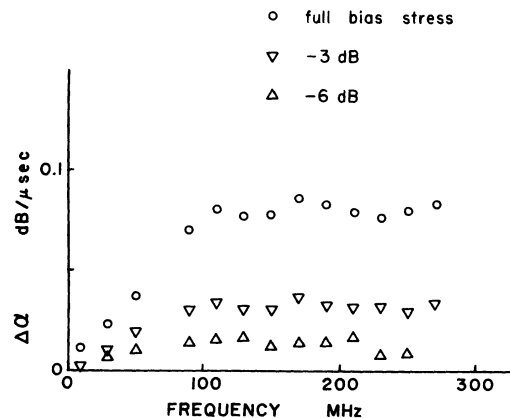


FIG. 3. Effect of the amplitude of the bias stress on $\Delta\alpha - \nu$ relation. The amplitude of the bias stress is reduced by 3 dB (∇) and 6 dB (Δ) from the full bias stress amplitude (\circ). $T=4.2^\circ\text{K}$.

were not changing significantly with temperature below 70 °K, even down to 2 °K. Second, the $\Delta\alpha - \nu$ relation observed at low temperatures shows that $\Delta\alpha$ becomes independent of frequency at high frequencies. This behavior cannot be accounted for by viscous damping.

We have examined, therefore, the following three loss mechanisms: (i) point defect dragging,^{10,11} (ii) drag due to charge cloud,^{12,13} and (iii) radiation damping. It is found that our experimental results cannot be accounted for by the first two mechanisms. Consequently, we have concentrated on radiation damping as the most likely source of dissipation, in terms of consistency with the experimental results.

B. Motion of a kink

Before we go into details of the analysis, the following features of kink motion are considered for subsequent references.

The glide motion of a dislocation may be considered to consist of two elemental processes. One is the creation and annihilation of kinks on the dislocation and the other is the motion of kinks along the dislocation. The former process involves the Peierls stress σ_P and the energy $U(\sigma)$ to form a pair of kinks in the presence of an applied stress. If the applied stress is larger than the Peierls stress, kinks will be created without thermal assistance. The Peierls stress in sodium chloride has been calculated to be in the order of $10^{-3}\mu$,¹⁴ where μ is the shear elastic constant. The stress amplitude σ_0 of the measuring wave used in this experiment is at most $10^{-6}\mu$. Therefore the measuring wave is not large enough to create kinks without thermal activation. The activation energy $U(\sigma)$ for creation of a pair of kinks may be calculated by¹⁵

$$U(\sigma) = U_k \left(1 + \frac{1}{4} \ln \frac{16\sigma_P}{\pi\sigma_0} \right) \text{ for } \sigma \ll \sigma_P$$

with

$$U_k = (2a/\pi)(2Cab\sigma_P/\pi)^{1/2},$$

where U_k is the energy of a kink, a is the interatomic spacing, b is Burgers's vector, and C is the line tension. For $\sigma_P/\mu = 10^{-3}$, $\sigma_P/\sigma_0 = 10^3$, and $C = \frac{1}{2}\mu b^2$, $U(\sigma)$ becomes 4.8×10^{-13} erg or 0.3 eV. The temperature at which the frequency of the creation of pairs of kinks becomes equal to the lowest frequency (10 MHz) of our measuring wave is then approximately 340 °K (using $\nu_0 = 3 \times 10^{11}$ /sec as the preexponential factor.)¹⁶ This means that in the temperature range considered here the probability to create kink pairs by the ultrasonic wave is very small, even with the assistance of thermal activation. For the second process, i. e., the motion of kinks along dislocations, the stress needed to move a kink in the absence of thermal activation (kink stress) σ_k and the activation energy W_k for kink mo-

tion (kink energy barrier) should be examined. According to Schottky,¹⁷ the two quantities may be expressed, respectively, by

$$\frac{\sigma_k}{\mu} = \frac{192}{\pi^2 \sqrt{3}} \left(\frac{1-\eta}{1+\eta} \right) \frac{b}{w} \left(\frac{\sigma_P}{\mu} \right)^2, \quad (1)$$

and

$$W_k = \frac{1}{5}(\sigma_k b^3), \quad (2)$$

where η is Poisson's ratio and w is the width of the kinks. For the values used before, together with $\eta = \frac{1}{3}$, and $b/w = \frac{1}{5}$, one obtains $\sigma_k/\mu = 10^{-6}$ and $W_k = 1.6 \times 10^{-18}$ erg or 0.01 °K. Sanders's¹⁸ calculation also indicates that $\sigma_k/\sigma_P = 10^{-2}$ and W_k is a small fraction of 1 °K. All these estimates indicate that even at 2 °K, which is the lowest temperature used in this investigation, there is enough thermal assistance for a kink to jump to the next potential valley. Recent experiments¹⁹ indicate that dislocation motion occurs in LiF at 0.1 °K under the effect of propagating thermal phonons, thus further supporting the validity of the above estimates.

The foregoing argument suggests that the dislocation contributions to the ultrasonic attenuation measured in this study are originating from the motion of builtin kinks (geometrical kinks).

C. Motion of a kink chain

The above analysis for the motion of kinks applies only to an isolated (free) kink. It may be more realistic, however, to consider a kink chain consisting of geometrical kinks of one sign shown in Fig. 4. In such a case the interaction energy between kinks as well as the entropy of the kink chain have to be taken into account for the analysis of the equilibrium positions of individual kinks. This problem has been treated in detail by Alefeld.²⁰ According to his analysis, however, the entropy term can be neglected for angles satisfying the following condition:

$$\sin\phi \gg 20\pi kT/(\mu ab^2\beta \ln n), \quad (3)$$

where

$$\beta = \left(\frac{1+\eta}{1-\eta} \right) \cos^2\phi + \left(\frac{1-2\eta}{1-\eta} \right) \sin^2\phi, \quad (4)$$

n is the number of kinks in the chain, and ϕ is the angle between the average dislocation line direction

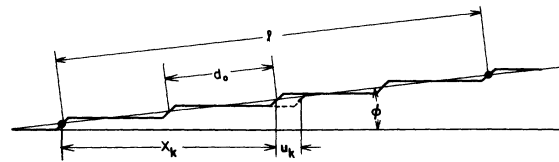


FIG. 4. Dislocation kink chain.

and a close-packed crystal direction. With $\eta = \frac{1}{3}$, the value of β ranges from $\frac{1}{2}$ for edge dislocations to 2 for screw dislocations. With the values of $\mu = 1.26 \times 10^{11}$ dyn/cm², $a = 5.63 \times 10^{-8}$ cm, $b = 4 \times 10^{-8}$ cm, and of Alefeld's estimate $\beta(\ln n)/4\pi = \frac{1}{4}$, one finds, for $T = 4.2$ °K,

$$\phi \gg 0.001.$$

Namely, the entropy term becomes important only for the kink chain making very small angles with the close-packed direction. On this basis, therefore, the entropy is disregarded in the following analysis.

The interaction energy between kinks has been calculated by several investigators,²¹⁻²³ and is given by

$$H(d) = \mu a^2 b^2 / 8\pi d \equiv c' / 2d, \quad (5)$$

where d is the separation distance between kinks. Equation (5) is a long-range interaction law and is only valid when d is large compared with the kink width. The kink energy barrier W_k mentioned before is then thought to be superimposed on this long-range interaction energy. When the entropy term is neglected, the kinks are uniformly spaced within a given kink chain pinned at both ends and the spacing d depends only on the angle ϕ (Fig. 4). Under an applied stress σ , which is much less than the kink stress σ_k , the jump frequency ν_0 of a kink to cross the kink barrier and to initiate kink motion may be calculated by the standard method of rate theory:

$$\begin{aligned} \nu_0 &= \nu_{12} - \nu_{21}, \\ \nu_{12} &= \nu_{00} \exp \left\{ - \left[W_k - \frac{1}{2} \sigma a b^2 + \frac{c'}{2} \right. \right. \\ &\quad \left. \left. \times \left(\frac{1}{d_0 - a} - \frac{1}{d_0} + \frac{1}{d_0 + a} - \frac{1}{d_0} \right) \right] / kT \right\}, \\ \nu_{21} &= \nu_{00} \exp \left\{ - \left[W_k + \frac{1}{2} \sigma a b^2 + \frac{c'}{2} \right. \right. \\ &\quad \left. \left. \times \left(\frac{1}{d_0} - \frac{1}{d_0 - a} + \frac{1}{d_0} - \frac{1}{d_0 + a} \right) \right] / kT \right\}, \end{aligned}$$

where d_0 is the initial (before stress is applied) separation between kinks, ν_{12} and ν_{21} are forward and backward jump frequencies, respectively, and ν_{00} is the attempt frequency. Since W_k , σb^2 , and $c'a^2/d_0^3$ is much less than kT , ν_0 can be approximated by

$$\nu_0 \approx \nu_{00} [(\sigma a b^2 - 2c'a^2/d_0^3)/kT]. \quad (6)$$

The above derivation of ν_0 may not be accurate because the Einstein frequency is used as the frequency factor. Nonetheless, it suggests that, upon application of a stress σ , not all the kinks can move, but only the kinks which satisfy the condition

$$\sigma a b^2 > 2c'a^2/d_0^3 \quad (7)$$

can start to move. It can be shown further that once one of the kinks in the chain goes across the kink barrier, the rest of the kinks in the chain will follow. Therefore, the chances for kink motion in a chain of n kinks should be enhanced by a factor n , provided the stress satisfies the condition given by Eq. (7). From these arguments, it follows that since there must exist a distribution of d_0 in a crystal the number of kinks which contribute to the energy dissipation when subjected to an oscillatory stress should depend on the amplitude of the applied stress σ_0 . The distribution of d_0 , however, is not known. Therefore we simply assume that the chains are evenly distributed with respect to the angle ϕ (rectangular distribution in terms of ϕ). Then the distribution function P for number of kinks in terms of a/d_0 becomes

$$P\left(\frac{a}{d_0}\right) d\left(\frac{a}{d_0}\right) = \left(\frac{\Lambda}{\phi_m a}\right) \left(\frac{a}{d_0}\right) d\left(\frac{a}{d_0}\right),$$

where ϕ_m is the largest angle of ϕ considered ($\phi \approx \sin \phi = a/d_0$). (It is assumed that all the chains have equal length l .) Then the total number of kinks per unit volume N is given by

$$N = \Lambda \phi_m / 2a,$$

where Λ is the total length of dislocations per unit volume. The number of kinks γ which will contribute to the energy dissipation under an applied stress of amplitude σ_0 then becomes

$$\gamma = \int_0^x P n d\left(\frac{a}{d_0}\right) = \left(\frac{\sigma_0}{\sigma_m}\right) N, \quad (8)$$

where $x = (\sigma_0 a^2 b^2 / 2c')^{1/3}$ and σ_m is the stress at which all the kinks (up to the ones having the maximum angle ϕ_m) move. It should be noted that Mason²⁴ derived a similar expression for γ from a different reasoning.

Once the kink motion is initiated, i. e., a kink goes across the first kink barrier, W_k , the kink acquires a kinetic energy by converting the potential energy W_k , and can cross the next and the subsequent energy barriers indefinitely if no other forces act on the kink. In practice, however, the kink experiences forces arising from the kink-kink interactions just mentioned, as well as a dynamic resistive force which is the source of the energy dissipation to be discussed later. Therefore, after crossing the first energy barrier, the motion of individual kinks should be described by a set of equations of motion

$$m \ddot{\chi}_k + f_1(\dot{\chi}_k) = \sigma a b + \sum_{l \neq k} f(\chi_k - \chi_l),$$

where χ_k is the coordinate of the k th kink, $f_1(\dot{\chi}_k)$ is the dynamic resistive force, and $f(\chi_k - \chi_l)$ is the interaction force between k th and l th kink.

The interaction force $f(d)$ can be derived from Eq. (5) (only nearest-neighbor interactions are considered here)

$$f(d) = \frac{\partial H}{\partial d} = \frac{\mu b^2}{8\pi} \left(\frac{a^2}{d^2} \right) \beta .$$

Since this force is nonlinear in d , a further approximation is made by expanding it in terms of $(d - d_0)$. The result²³ to first order is then

$$f(u_k) = -c(u_{k-1} - 2u_k + u_{k+1}) , \quad (9)$$

where u_k is the displacement of the k th kink from its equilibrium position, and c is given by

$$c = \mu a^2 b^2 \beta / 4\pi d_0^3 . \quad (10)$$

In the case of viscous damping, the resistive force is given by $B\dot{u}_k$, B being the viscous damping coefficient, and the set of the equations of motion takes the form

$$m\ddot{u}_k + B\dot{u}_k + c(u_{k-1} - 2u_k + u_{k+1}) = \sigma ab . \quad (11)$$

Suzuki and Elbaum²⁵ showed that the expression of attenuation α for such a system has exactly the same form (in terms of resonant frequency ω_0 , applied frequency ω and B) as that derived from the string model with viscous damping.²⁶ It is obvious, therefore, that the kink model with viscous damping does not account for the present results. However, for the purposes of subsequent references, steps leading to the expression for attenuation α for this case are listed in the Appendix.

D. Radiation damping

Eshelby²⁷ showed that when a kink oscillates, energy is dissipated through radiation of elastic waves. His expression for the dynamic resistive force is

$$f_1(\dot{\chi}) = \gamma_1 \ddot{\chi} ,$$

with

$$\gamma_1 = \mu a^2 b^2 / 10\pi c_r^3$$

and

$$1/c_r^3 = (1/c_l^3) [1 + \frac{2}{3}(c_l^5/c_t^5)] ,$$

where c_l and c_t are the velocities of longitudinal and shear waves, respectively. If one uses this as the dynamic resistive force, the expression for the attenuation takes the form

$$\alpha \propto \frac{\gamma_1 \omega^4}{(\omega_0^2 - \omega^2)^2 + \gamma_1^2 \omega^6} .$$

Obviously this does not provide the frequency dependence needed to explain the observed results.

Eshelby's treatment is based on a continuum model and does not take into account the effect of energy barriers for kink motion. Consequently, in order to radiate energy, a kink has to be driven by

an applied time varying force such as an oscillatory stress. When the kink barriers are included, the kink motion is not expected to be smooth and may be accelerated and decelerated in crossing the barriers, even if the average velocity v is kept constant (applied stress is not necessarily oscillatory in contrast to the continuum model). Such a change in velocity also is a source of energy radiation. This problem has been treated by several investigators including Hart²⁸ and Nabarro.²⁹ Recently Alshits *et al.*³⁰ made a detailed calculation of this problem and showed that, at high average kink velocities, a kink emits energy mainly on the fundamental frequency, and that the radiation damping is proportional to $1/v$. With decreasing velocity, the increase in the degree of nonuniformity of the kink motion results in a broadening of the radiation spectrum and in the growth of the dissipation. The decrease of the velocity is possible only up to some critical velocity v_c , below which a steady-state kink motion is not realized.

Suzuki³¹ also considered this problem from the analogy between charged particles in an electric field and dislocations in a stress field. According to his calculation, the stress required to move dislocations with a certain velocity v over an energy barrier W is given by

$$\sigma \approx \frac{\pi \rho b l}{8a^2 c_t} \left(\frac{W}{M} \right)^2 \left(\frac{M}{\frac{1}{2} M v^2 + \frac{1}{2} W} \right)^{1/2} ,$$

where l is the length of the dislocation. If one applies this formula to the case of kink motion by replacing l with a (kink height), W by $\frac{1}{4}\sigma_k a b^2$, and with

$$M = \frac{2\mu a^2 b^2}{\pi \omega c_t^2} \quad (\text{kink mass}) ,$$

the following expression is obtained

$$\sigma = \sigma_k \frac{\pi}{16} \frac{b}{a} \left(\frac{\pi w}{4a} \right)^{3/2} \left(\frac{\sigma_k}{\mu} \right)^{1/2} \frac{1}{(1 + 8\mu a v^2 / \pi \sigma_k \omega c_t^2)^{1/2}} . \quad (12)$$

In one extreme case, i. e.,

$$\frac{8\mu a v^2}{\pi \sigma_k \omega c_t^2} \ll 1 ,$$

the above expression reduces to Alshits *et al.*'s³⁰ expression for the resistive force corresponding to the critical velocity v_c [Eq. (18) in Ref. 20]:

$$\sigma_{dPk} = \sigma_k \left(\frac{1}{10} \right) \frac{a}{b} \left(\frac{\pi w}{4a} \right)^{3/2} \left(\frac{\sigma_k}{\mu} \right)^{1/2} . \quad (13)$$

In the other extreme case, i. e.,

$$\frac{8\mu a v^2}{\pi \sigma_k \omega c_t^2} \gg 1 ,$$

Eq. (12) becomes

$$\sigma = \sigma_k \left(\frac{\sqrt{2} \pi^2}{8^3} \frac{b^2}{a^2} \right) \left(\frac{w^2}{ab} \right) \left(\frac{\sigma_k}{\mu} \right) \left(\frac{c_t}{v} \right), \quad (14)$$

which may be compared with the expression of Alshits *et al.*

$$\sigma = \sigma_k \left(\frac{\pi}{120} \right) \left(\frac{w^2}{ab} \right) \left(\frac{\sigma_k}{\mu} \right) \left(\frac{c_t}{v} \right).$$

Thus, both the analyses of Alshits *et al.* and Suzuki predict that at low velocities (below v_c), the resistive force for kink motion is independent of the kink velocity and given by σ_{dPk} , the dynamic Peierls stress³² for kinks; and at high velocities, the resistive force is inversely proportional to the kink velocity. If it is assumed that the critical velocity v_c is determined by the condition

$$\frac{8\mu av_c^2}{\pi \sigma_k w c_t^2} = 1,$$

then for values of $\sigma_k/\mu = 10^{-6}$ and $w = 5a$, v_c becomes $1.4 \times 10^{-3} c_t$. The distance a kink travels in the quarter cycle of the applied oscillatory stress is thought to be in the order of ten interatomic spacings. Then the critical velocity v_c can be achieved at a frequency of 150 MHz, which is well in our experimental frequency range.

According to this model, the kink will accelerate indefinitely (in the high velocity range) if the applied stress is the only stress acting on the kink. In order to prevent this from occurring, Alshits *et al.* introduced a large viscous damping without specifying its origin. It is difficult, however, to find such a large viscous damping at the low temperatures under discussion. We consider here, instead, the case of geometrical kink chains pinned at both ends. In this case, the interaction between kinks will prevent the divergence from occurring.

E. Attenuation due to radiation damping

In the following the attenuation and the modulus defect (in terms of the velocity change) caused by the radiation mechanism just mentioned are presented. Only the two limiting cases are treated in detail.

1. Low velocity region

In this region the dynamic resistive force is independent of kink velocity:

$$F = \sigma_{dPk} ab. \quad (15)$$

In order to incorporate the velocity-independent dynamic resistive force into the equation of motion, we use the "equivalent viscous damping method",³³ which postulates the equivalence of work done by the real force $\sigma_{dPk} ab (\equiv B_1)$ and by the equivalent (fictitious) viscous damping force $b_1 \dot{u}_k$ at the end of each cycle;

$$4 \int_0^{\pi/2\omega} B_1 \left(\frac{du_k}{dt} \right) dt = 4 \int_0^{\pi/2\omega} b_1 \left(\frac{du_k}{dt} \right)^2 dt$$

or

$$b_1 = \frac{4}{\pi} \left(\frac{B_1}{\omega u_{k0}} \right). \quad (16)$$

It should be noted that the equivalent damping coefficient b_1 depends on u_{k0} (the displacement amplitude of the k th kink) and no longer is a material constant. By substituting b_1 for B in the expression (A9) and solving it for u_{k0} , one obtains

$$u_{k0} = \left[K_k^2 - \left(\frac{4}{\pi} \frac{B_1}{M} \right)^2 \right]^{1/2} / (\omega_1^2 - \omega^2),$$

where

$$K_k = \left(\frac{2}{n+1} \right) \cot \left(\frac{\pi}{2} \frac{1}{n+1} \right) \left(\frac{\sigma_0 e^{-\alpha y} ab}{M} \right) \sin \frac{\pi k}{n+1}.$$

The displacement of the k th kink becomes

$$u_k = u_{k0} \cos[\omega t - (\omega/V)y - \psi_k]$$

with

$$\tan \psi_k = \frac{4}{\pi} \frac{B_1}{M} \left/ \left[K_k^2 - \left(\frac{4}{\pi} \frac{B_1}{M} \right)^2 \right]^{1/2} \right.$$

From these quantities, one obtains

$$\alpha = \frac{1}{2} \frac{1}{n+1} \frac{Nab\mu}{\sigma_0 e^{-\alpha y}} \left(\frac{\omega}{\omega_1^2 - \omega^2} \right) \times \sum_{k=1}^n \frac{4}{\pi} \frac{B_1}{M} \left[1 - \left(\frac{(4/\pi)(B_1/M)}{K_k} \right)^2 \right]^{1/2}, \quad (17)$$

$$\frac{\Delta V}{V} = \frac{1}{2} \frac{1}{n+1} \frac{Nab\mu}{\sigma_0 e^{-\alpha y}} \frac{1}{\omega_1^2 - \omega^2} \times \sum_{k=1}^n K_k \left[1 - \left(\frac{(4/\pi)(B_1/M)}{K_k} \right)^2 \right]. \quad (18)$$

The above expression for α loses meaning unless the following condition is fulfilled:

$$\left(\frac{(4/\pi)(B_1/M)}{K_k} \right)^2 < 1.$$

The relative magnitudes of K_k^2 and $[(4/\pi)(B_1/M)]^2$ are practically determined by $\{\sigma_0 \sin[\pi k/(n+1)]\}^2$ and $(\sigma_{dPk})^2$ (the factor $[2/(n+1)] \cot[\frac{1}{2}\pi/(n+1)]$ in K_k changes from 1 to $4/\pi$ as n increases from 1 to ∞). σ_0 is in the order of 10^4 dyn/cm² and σ_{dPk} is estimated to be 10^3 dyn/cm² ($\sigma_{dPk}/\sigma_k = 10^{-2}$, $\sigma_k/\mu = 10^{-6}$). If one sets a criterion

$$\left(\frac{\sigma_{dPk}}{\sigma_0 \sin[\pi k/(n+1)]} \right)^2 < 0.1$$

for $[(4/\pi)(B_1/M)]^2$ to be neglected against K_k^2 , 20 kinks out of 99 kinks of the chain (the first ten and the last ten kinks) fail to meet this criterion. For a kink chain containing less than nine kinks, all the kinks meet this criterion. Within this approxima-

tion, we may discard the term $[(4/\pi)(B_1/M)]^2$ against K_k^2 , and obtain

$$\alpha' \approx \frac{1}{2V} \left(\frac{n}{n+1} \right) \frac{4}{\pi} \left(\frac{Na^2 b^2 \mu \sigma_{dPk}}{\sigma_0 e^{-\alpha y} M} \right) \frac{\omega}{\omega_1^2 - \omega^2}, \quad (19)$$

$$\frac{\Delta V'}{V} \approx \frac{1}{2} \left(\frac{2}{(n+1)^2} \cot^2 \left(\frac{\pi}{2} \frac{1}{n+1} \right) \frac{Na^2 b^2 \mu}{M} \left(\frac{1}{\omega_1^2 - \omega^2} \right) \right). \quad (20)$$

In the above derivation, however, it is assumed that all the movable kinks N will contribute to the energy dissipation upon application of even an infinitesimal stress. As mentioned earlier, the number of kinks γ which participate in the energy dissipation depends on the amplitude of the applied stress σ_0 [expression (8)]. Therefore, N in the expressions (19) and (20) should be replaced by $(\sigma_0/\sigma_m)N$, and finally one obtains

$$\alpha \approx \frac{1}{2V} \left(\frac{n}{n+1} \right) \frac{4}{\pi} \left(\frac{Na^2 b^2 \mu \sigma_{dPk}}{\sigma_m M} \right) \frac{\omega}{\omega_1^2 - \omega^2}, \quad (21)$$

$$\frac{\Delta V}{V} \approx \frac{1}{2} \left(\frac{2}{(n+1)^2} \cot^2 \left(\frac{\pi}{2} \frac{1}{n+1} \right) \frac{\sigma_0 e^{-\alpha y} Na^2 b^2 \mu}{\sigma_m M} \left(\frac{1}{\omega_1^2 - \omega^2} \right) \right). \quad (22)$$

As can be seen, as long as the frequency of the applied stress ω is much smaller than the resonant frequency ω_1 , the attenuation α increases linearly with frequency and does not depend on the amplitude of the measuring wave, while the velocity change $\Delta V/V$ is independent of the frequency ω but increases with the amplitude of the wave. It should be noted also that, for a given chain length l , the contributions of each individual kink to the attenuation α (and also to $\Delta V/V$) are approximately the same regardless of the kink density n , therefore of angle ϕ , provided n is not too small. Qualitatively, this is because, for a given chain length, as the angle ϕ decreases the number of kinks n decreases, but the distance each kink travels during the stress cycle is larger, and the area swept out by the chain, which is the measure of the energy dissipation, does not depend strongly on the angle ϕ . This is not the case for the viscous-type damping because the area swept out by the chain is not directly proportional to the energy dissipation.

The quantities we measure, however, are not the attenuation α nor $\Delta V/V$ themselves, but the change of these quantities $\Delta\alpha$ and $\Delta(\Delta V/V)$, due to the dynamic bias stress. The role of the bias stress has been thought to be a slight increase of loop length l , on the average, by depinning dislocations from weak pinning points, as described in Ref. 7. However, in case of a system of kink chains, the effect of the bias stress may be better understood in terms of increasing the number of kinks responsible for the energy dissipation, by activating kink chains having larger angles which would not be activated by the measuring wave alone. Namely, the number of kinks γ is increased from

$(\sigma_0/\sigma_m)N$ to $[(\sigma_0 + \frac{1}{2}\sigma_B)/\sigma_m]N$, where σ_B is the amplitude of the bias stress, and the factor $\frac{1}{2}$ arises from the fact that, in our present experimental arrangement, two out of four slip systems the measuring wave activates are affected by the bias stress. Then the incremental attenuation and the corresponding velocity change become, respectively,

$$\Delta\alpha \approx \frac{1}{4V} \left(\frac{n}{n+1} \right) \frac{4}{\pi} \left(\frac{\sigma_B Na^2 b^2 \mu \sigma_{dPk}}{\sigma_m \sigma_0 e^{-\alpha y} M} \right) \frac{\omega}{\omega_1^2 - \omega^2}, \quad (23)$$

$$\Delta \left(\frac{\Delta V}{V} \right) \approx \frac{1}{4} \left(\frac{2}{(n+1)^2} \cot^2 \left(\frac{\pi}{2} \frac{1}{n+1} \right) \left(\frac{\sigma_B Na^2 b^2 \mu}{\sigma_m M} \right) \frac{1}{\omega_1^2 - \omega^2} \right). \quad (24)$$

It is clear from the above expression that the frequency characteristics remain the same as before, but $\Delta\alpha$ has an "inverse" amplitude dependence (i. e., the incremental attenuation decreases as the amplitude of the measuring wave increases), while $\Delta(\Delta V/V)$ is insensitive to the measuring wave amplitude.

Evidence for the "inverse" amplitude dependence is presented in Fig. 5. Here the measuring wave amplitudes of each frequency indicated are increased by 10 dB, in 1-dB steps, while the amplitude of the bias stress is kept constant throughout the experiments. It is apparent that the magnitude of the "inverse" amplitude dependence seems to increase as the measuring wave frequency increases, in accordance with the prediction of expression (23). When the amplitude dependence experiments are conducted without the bias stress, either no amplitude dependence or very slight "normal" amplitude dependence is detected. This inverse amplitude dependence is influenced markedly by the temperature at which the experiments are conducted. An example for this is shown in Fig. 6.

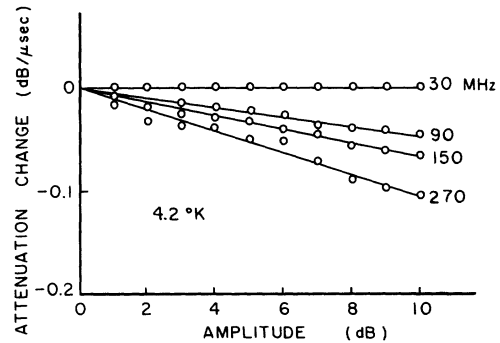


FIG. 5. Attenuation change as a function of measuring wave amplitude, at frequencies of 30, 90, 150, and 270 MHz, in the presence of a bias stress (same for each frequency). The amplitude of the measuring wave is increased by 10 dB in 1-dB steps. The attenuations are normalized to the value corresponding to the lowest amplitude at each frequency. $T = 4.2^\circ\text{K}$.

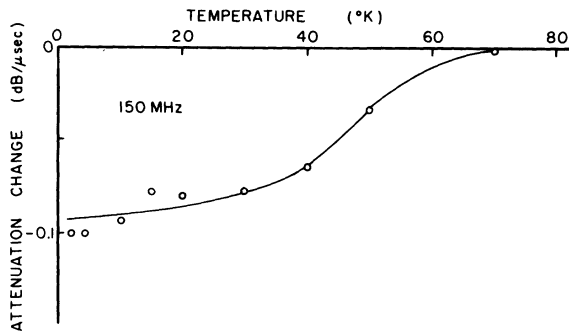


FIG. 6. Effect of temperature on "inverse" amplitude dependence. $\nu = 150$ MHz. The attenuation decrease due to 10 dB increases in the 150-MHz measuring wave in the presence of a bias stress (same for all temperatures) is plotted as a function of temperature.

As can be seen, the effect decreases as temperature increases, and at 70 °K, the inverse amplitude dependence disappeared. Again, without the bias stress, no amplitude dependence was detected throughout the temperature range tested.

The inverse amplitude dependence was predicted earlier by Suzuki and Elbaum²⁵ and by Alefeld.^{20,34} The origin of this effect (nonlinearity) in their theories, however, is the higher-order terms in the interaction force between kinks, and is not the nonlinear damping terms discussed here (a viscous-type damping is used in their theories). Nonlinearity in the interaction force, however, fails to explain the present experimental results at least in two accounts: (i) the frequency dependence of $\Delta\alpha$, and (ii) the sign of $\Delta\alpha$. The first point was already mentioned earlier. For the second point, the nonlinear interaction force mechanism predicts $\Delta\alpha$ to be negative,³⁴ while we have never observed negative $\Delta\alpha$ throughout our experiments.

Figure 7 shows the results of concurrent measurements of $\Delta\alpha$ and $\Delta(\Delta V/V)$ taken at frequencies of 15, 45, 75, and 105 MHz and at a temperature of 4.2 °K. In accordance with the predictions of the expressions (23) and (24), $\Delta\alpha$ increases linearly with frequency, while $\Delta(\Delta V/V)$ appears to be independent of frequency, though there is substantial scatter in the experimental points. Using a pair of experimental values of $\Delta\alpha$ and $\Delta(\Delta V/V)$ [for example, $\Delta\alpha = 0.03$ dB/ μ sec, and $\Delta(\Delta V/V) = 2 \times 10^{-5}$ at 75 MHz], one can calculate the ratio σ_{dPk}/σ_0 from the expressions (23) and (24):

$$\frac{\Delta\alpha}{\Delta(\Delta V/V)} \approx \frac{\omega}{c_t} \left(\frac{\sigma_{dPk}}{\sigma_0} \right) \frac{\pi}{2},$$

or $\sigma_{dPk}/\sigma_0 \approx 1.2 \times 10^{-1}$. Since the stress amplitude of the measuring wave σ_0 is in the order of 10^4 dyn/cm² or $10^{-7}\mu$, σ_{dPk} should be in the order of

$10^{-8}\mu$, which agrees with the theoretical estimate $\sigma_{dPk}/\sigma_k = 10^{-2}$ by Weiner,³² combined with $\sigma_k/\mu = 10^{-6}$ by Schottky.¹⁷

In the following, dislocation attenuation α is estimated from the expression (21) and from the corresponding expression of the string model with viscous damping²⁶ (attributed here to phonon scattering) which may be written as

$$\alpha = \frac{4\mu b^2 \Lambda}{\pi^2 A V} \frac{\omega^2 B/A}{(\omega_0^2 - \omega^2)^2 + (\omega B/A)^2}, \quad (25)$$

$$\omega_0 = (\pi/l)(C/A)^{1/2}, \quad C = \frac{1}{2}\mu b^2, \quad A = \pi\rho b^2.$$

With numerical values of $\mu = 1.26 \times 10^{11}$ dyn/cm², $a = 5.6 \times 10^{-8}$ cm, $b = 4 \times 10^{-8}$ cm, $c_t = 2.4 \times 10^5$ cm/sec, $V = 4.5 \times 10^5$ cm/sec, and with the estimated values of $\sigma_B/\sigma_m = 10^{-1}$, $l = 10^{-4}$ cm, $d_0 = 10^{-6}$ cm, $n \approx n+1 = l/d_0 = 10^2$, $\Lambda = 10^6$ cm/cm³, $N = \Lambda/d_0 = 10^{12}$ and with $\sigma_{dPk}/\sigma_0 = 10^{-1}$ (just obtained above), $\Delta\alpha$ [Eq. (23)] is calculated to be 4×10^{-2} Np/cm or 1.6×10^{-1} dB/ μ sec for 100 MHz, which is comparable to the data shown in Figs. 1–3. The dislocation attenuation α due to the radiation mechanism is then estimated to be in the order of 3×10^{-2} dB/ μ sec ($\alpha = \Delta\alpha \times 2\sigma_0/\sigma_B$). On the other hand, the calculation from the expression (25) at the same frequency and with the same values of the parameters yields $\alpha \approx 10^{-6}$ Np/cm or 4×10^{-6} dB/ μ sec. In this calculation, the viscous damping constant B is estimated from the assumption that B is proportional to the thermal energy density, and is scaled down to 4.2 °K from the measured value⁷ of 10^{-5} dyn sec/cm² at 70 °K (with Debye temperature $\Theta_D = 321$ °K). It is concluded from these estimates that the observed dislocation damping at low temperatures cannot be attributed to phonon scattering in the sense formulated to date, and applicable at higher

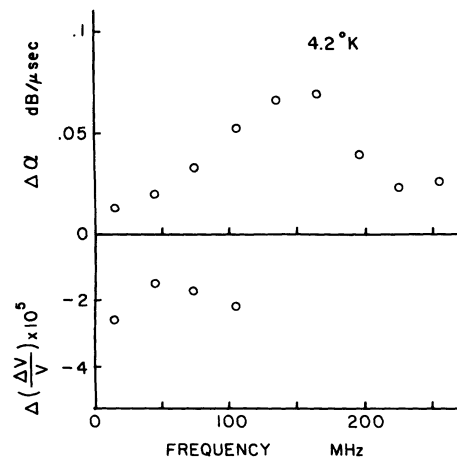


FIG. 7. Concurrent measurement of attenuation change $\Delta\alpha$ and the velocity change $\Delta(\Delta V/V)$ as a function of frequency. $T = 4.2$ °K.

temperatures.^{6,7}

The concept of using a dynamic Peierls stress of a kink, σ_{dPk} , as the source of internal friction, was introduced previously by Mason.^{24,35,36} In his treatment, however, the dynamic resistive force arising from σ_{dPk} is set to be proportional to the applied stress σ , i. e.,

$$F = (\sigma_{dPk}/\sigma_k) b\sigma(t)$$

for unit length of dislocation. Thus the equation of motion remains linear as in the case of the viscous damping, and no amplitude dependence appears in either attenuation or modulus defect. Consequently, such a treatment presents difficulties in explaining the "inverse" amplitude dependence observed in $\Delta\alpha$ mentioned above.

2. High velocity region

In this region the resistive force is inversely proportional to the kink velocity;

$$F = Qab/v,$$

where

$$Q = \sigma_k \left(\frac{\sqrt{2}\pi^2 b^2}{8^3 a^2} \right) \left(\frac{\omega^2}{ab} \right) \left(\frac{\sigma_k}{\mu} \right) c_t.$$

Here again the equivalent viscous damping method is used. The equivalent damping coefficient q becomes

$$q = 2Qab/u_{k0}^2 \omega^2. \quad (26)$$

The amplitude u_{k0} and phase angle ψ_k are given by

$$u_{k0} = \frac{K_k + [1 - (2(\omega_1^2 - \omega^2)2Qab/K_k^2 M\omega)]^{1/2}}{\sqrt{2}(\omega_1^2 - \omega^2)},$$

$$\tan\psi_k = (2Qab/M\omega u_{k0}^2)/(\omega_1^2 - \omega^2),$$

which leads to

$$\alpha = \frac{1}{2c_t} \left(\frac{NabQ\mu}{\sigma_0 e^{-\alpha y} \sigma_m} \right) \tan\left(\frac{\pi}{2} \frac{1}{n+1}\right) \times \sum_{m=1}^n \frac{1}{\sin[\pi m/(n+1)]}, \quad (27)$$

$$\frac{\Delta V}{V} = \frac{1}{2} \left(\frac{\sigma_0 e^{-\alpha y} Na^2 b^2 \mu}{M\sigma_m} \right) \frac{2}{(n+1)^2} \cot^2\left(\frac{\pi}{2} \frac{1}{n+1}\right) \frac{1}{\omega_1^2 - \omega^2}. \quad (28)$$

The effect of the bias stress is again thought to increase the number of participating kinks, and one obtains

$$\Delta\alpha = \frac{1}{4c_t} \left(\frac{\sigma_B NabQ\mu}{(\sigma_0 e^{-\alpha y})^2 \sigma_m} \right) \tan\left(\frac{\pi}{2} \frac{1}{n+1}\right) \times \sum_{m=1}^n \frac{1}{\sin[\pi m/(n+1)]}, \quad (29)$$

$$\Delta\left(\frac{\Delta V}{V}\right) = \frac{1}{4} \frac{\sigma_B Na^2 b^2 \mu}{M\sigma_m} \frac{2}{(n+1)^2} \cot^2\left(\frac{\pi}{2} \frac{1}{n+1}\right) \frac{1}{\omega_1^2 - \omega^2}. \quad (30)$$

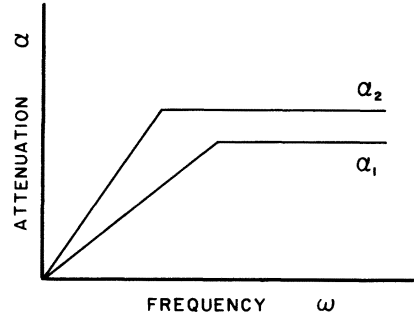


FIG. 8. Schematic representation of attenuation as a function of frequency, α_1 without bias stress, α_2 in the presence of a bias stress.

As can be seen, $\Delta\alpha$ is independent of the frequency ω , which is consistent with the experimental observation at high frequencies. It should be noted that α and $\Delta\alpha$ are independent of the resonant frequency ω_1 , and are proportional to $1/\sigma_0$ and $1/\sigma_0^2$, respectively. This last characteristic indicates that in this high velocity region, α itself has the inverse amplitude dependence, and when a bias stress is applied, the effect should be enhanced. The experimental verification of this matter was not possible because of the insufficient dynamic range of our attenuation measurement instrument, when operated at high frequencies.

Another feature of the experimental results shown in Figs. 1 and 2 is a small "hump" in the $\Delta\alpha - \nu$ relation which sometimes appears in the transition region between the frequency-dependent and frequency-independent regions. This hump is thought to arise from the effect illustrated schematically in Fig. 8. In this figure, α_1 portrays the frequency dependence of the attenuation in the absence of a bias stress, according to Eqs. (21) and (27), with emphasis on the linear dependence of α on ν and the ν -independent regions. The application of a bias stress causes α to change from α_1 to α_2 . If the transition between the two regions appears at lower frequencies when a bias stress is applied, then since the measured incremental attenuation $\Delta\alpha$ is the difference between α_2 and α_1 , $\Delta\alpha$ will display all the qualitative features, including the hump. Under what conditions the shift of the transition to lower frequencies occurs is yet to be explored. Alternatively, the hump may indicate the onset of the singularity $\omega_0^2 = \omega^2$, which does not fully develop, because the frequency-independent attenuation takes over.

The velocity change $\Delta(\Delta V/V)$, on the other hand, contains a factor $(\omega_1^2 - \omega^2)$ and does not depend on σ_0 . Therefore, there should be no amplitude dependence, and at high frequencies the effect of a singularity should be observed. Unfortunately, our velocity measurement technique is limited to the

frequency of up to 110 MHz at present. Therefore, full confirmation of the validity of the model used is still subject to verifying the above predictions.

The experimental results at high frequencies (i. e., attenuation independent of frequency), imply that the decrement (energy dissipated per cycle) is inversely proportional to frequency. On the other hand, for a given amplitude of an oscillatory stress, the dislocation (or kink) velocity is proportional to the frequency. Therefore, this behavior can be interpreted in terms of a dynamic resistive force which is inversely proportional to the dislocation (kink) velocity. The radiation mechanism just discussed, however, is not the only mechanism having such characteristics. In the theory of phonon viscosity proposed by Mason,³⁷ Suzuki *et al.*³⁸ suggested that the cutoff radius $r(=\frac{3}{4}b)$ should be replaced by $r^* = v\bar{l}/V$ when r^* becomes larger than r . Here, V is the Debye average velocity of sound, v is the velocity of dislocation, and \bar{l} is the phonon meanfree path. Since the expression for the damping constant (viscous) derived by Mason is proportional to $1/r^2$, use of r^* given above causes the resistive force to be inversely proportional to the dislocation velocity. However, the concept of applying the phonon viscosity, which was originally proposed as a mechanism for ultrasonic attenuation, to dislocation damping is questionable and often criticized.^{3,4} In fact, our experimental results shown in Refs. 6 and 7 indicate clearly that this is not the case (the temperature dependence of B is too steep to be accounted for by the phonon viscosity theory).

Seeger and Engelke³⁹ discussed the Lorentz contraction of dislocation width as a possible cause of decrease in resistive force at high dislocation velocities. The maximum resistive force takes place, according to their theory, at a velocity approximately $\frac{3}{4}$ of the sound velocity, which is considered to be much too high for the present experiments. In any case, their theory concerns the scattering of phonons from dislocation strain fields and therefore is not relevant at the temperatures under discussion.

Ookawa and Yazu⁴⁰ derived a resistive force inversely proportional to dislocation velocity arising from the radiation caused by velocity fluctuations similar to the one discussed here. However, the velocity fluctuations these authors considered are the acceleration (and deceleration) of uniformly moving dislocations encountering a strain field of an isolated defect. Therefore, their calculation pertains to an "extrinsic" loss in which dislocations must travel considerable distances before this mechanism becomes operative.

Finally, we examine the connection between the low-temperature mechanisms discussed here and the viscous damping assumed to prevail at higher

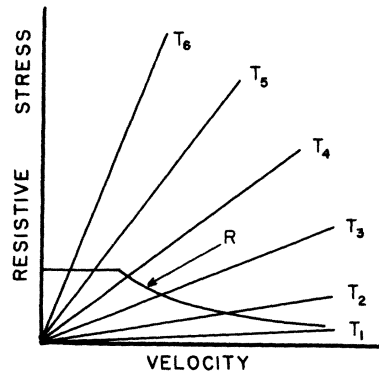


FIG. 9. Proposed (schematic) dependence of resistive force acting on dislocation (or kink) as a function of dislocation (or kink) velocity. Straight lines labeled T_1 to T_6 represent the case of viscous damping for increasing temperature ($T_1 < T_2 < \dots < T_6$). Curve labeled R represents the case of radiation damping and of the type discussed in the text.

temperatures (i. e., $T > 70^\circ\text{K}$). Figure 9 shows schematically the proposed resistive force dependence on velocity, for various temperatures. The straight lines labeled T_1 to T_6 are assumed to represent the resistance due to viscous damping as the temperature increases from T_1 to T_6 (the slope of the straight line is the damping coefficient B). The curve R , composed of a velocity-independent region at low velocities, and a part proportional to the reciprocal of the velocity at high velocities, represents the resistance due to radiation damping, as discussed above (it is assumed that to a first approximation this curve is independent of temperature). The transition from high- to low-temperature behavior is viewed as follows. At any set of conditions, the largest values of the resistive force dominates; thus at high temperatures (say, T_6) and all but the smallest velocities, viscous damping applies. As the temperature is lowered, the viscous damping becomes less and less important for a given velocity. At the lowest temperatures viscous damping becomes negligible for all velocities and radiation damping dominates throughout. This behavior could also account for the fact that dislocation damping measured at low frequencies (KHz region and below) generally displays a frequency-independent decrement and is therefore not consistent⁴¹⁻⁴³ with the predictions of the Granato-Lücke theory,²⁶ which is based on viscous damping only. Indeed, at low frequencies the dislocation velocities are generally small and could be in the region to the left of the viscous damping line that corresponds to the temperature of the experiment. Under these conditions the damping would be governed by the radiation loss depicted by the curve R , and would display the feature mentioned above. Furthermore, it is worth noting that in the irradiation

experiments concerning the dislocation pinning rate determination, investigators^{44,45} prefer to use, for various reasons, the modulus defect data (velocity change data) rather than the decrement data (attenuation data). If the condition of such an experiment falls into the regime where the radiation damping discussed here predominates, a viscous damping model will provide incorrect loop length dependence (l^4 dependence instead of l^2) for the decrement. On the other hand, as far as the modulus defect is concerned, it is irrelevant whether one uses the viscous damping model or the radiation damping model, because the loop length dependence is the same (l^2 dependence) for the two models.

IV. CONCLUSIONS

It is shown that, among the mechanisms so far investigated, the radiation damping of the type discussed here is the only mechanism which can explain the experimental results concerning the magnitude and frequency dependence of the incremental attenuation $\Delta\alpha$ of sodium chloride taken at low temperatures. The radiation mechanism considered here originates from the fluctuations of velocity when a kink moves across the energy barriers arising from the discrete lattice structure of the crystal, and has the characteristics such that, when the average velocity of the kink is small, the dynamic resistive force against the kink motion is independent of the velocity, and at high average velocities of the kink, the resistive force becomes inversely proportional to the velocity. These dynamic characteristics are incorporated with the static interaction forces between kinks in a system of kink chains, and the expressions for the attenuation α and velocity change ($\Delta V/V$) as well as the incremental changes of these caused by a dynamic bias stress, $\Delta\alpha$ and $\Delta(\Delta V/V)$, are presented. The predictions of the analysis such as the frequency dependence of $\Delta\alpha$ ($\Delta\alpha$ increases linearly with frequency at low frequencies and becomes independent of frequency at high frequencies), and the amplitude dependence (no amplitude dependence in α but "inverse" amplitude dependence in $\Delta\alpha$ in low-frequency region) are verified by experiments. By measuring concurrently the $\Delta\alpha$ and $\Delta(\Delta V/V)$ in the low-frequency region, the dynamic Peierls stress for kinks, σ_{dPk} , is determined to be in the order of 10^3 dyn/cm². The relation between the radiation damping mechanism and the viscous damping mechanism which prevails at high temperatures is discussed. A possible cause of the discrepancies between the Granato-Lücke theory and the low-frequency decrement experiments is suggested.

ACKNOWLEDGMENTS

The authors are pleased to acknowledge stimulating discussions with Professor J. H. Weiner on the

subject of dislocation kink dynamics and help from Dr. J. Deputat with the early stages of the experimental work.

APPENDIX

Calculation of attenuation and velocity change for a system of kink chains of n kinks with viscous damping ($F = Bv$) pinned at both ends. We follow the method of Granato-Lücke²⁶ used for vibrating string model.

The linearized differential equation of a kink

$$M\ddot{u}_k + B\dot{u}_k + c(u_{k-1} - 2u_k + u_{k+1}) = b\sigma(y, t), \quad (A1)$$

and the equation of motion for a propagating wave (in the y direction)

$$\frac{\partial^2 \sigma}{\partial y^2} - \frac{\rho}{\mu} \left(\frac{\partial^2 \sigma}{\partial t^2} \right) = \frac{\Lambda \rho a b}{l} \left(\frac{\partial}{\partial t^2} \right) \sum_{k=1}^n u_k(y, t),$$

$$k = 1, 2, \dots, n, \quad (A2)$$

should be solved simultaneously with the boundary conditions

$$u_0(y, t) = u_{n+1}(y, t) = 0. \quad (A3)$$

Here, M is the kink mass; u_k is the displacement of k th kink from its equilibrium position; B is the viscous damping constant; c is the linearized spring (interaction force) constant between kinks, given by expression (10); $\sigma(t)$ is the applied oscillatory stress; ρ is the density of the material; μ is the shear modulus; a is the interatomic spacing (kink height); b is Burgers's vector; Λ is the total length of movable dislocations per unit volume; and l is the length of the kink chain.

The set of equations (A1) can be decoupled²⁹ by the expression

$$u_k = \sum_{m=1}^n a_m(y, t) \left(\frac{2}{n+1} \right)^{1/2} \sin \left(\frac{\pi k m}{n+1} \right), \quad (A4)$$

and together with a trial solution of the form

$$\sigma = \sigma_0 e^{-\alpha y} \cos[\omega t - (\omega/V)y],$$

one obtains

$$a_m(y, t) = \left(\frac{2}{n+1} \right)^{1/2} \cot \left(\frac{\pi m}{2(n+1)} \right) \frac{\sigma_0 e^{-\alpha y} a b}{M}$$

$$\times \frac{\cos[\omega t - (\omega/V)y - \psi_m]}{\{(\omega_m^2 - \omega^2)^2 + [(B/M)\omega]^2\}^{1/2}},$$

$$\omega_m^2 = \frac{4c}{M} \sin^2 \left(\frac{\pi m}{2(n+1)} \right),$$

$$\tan \psi_m = \frac{(B/M)\omega}{\omega_m^2 - \omega^2},$$
(A5)

where σ_0 is the amplitude of the applied stress; α is the attenuation constant; ω is the angular frequency of the applied stress; and V is the wave velocity. The plastic strain ϵ due to these kink displacements becomes

$$\epsilon = \frac{\Lambda ab}{l} \sum_{k=1}^n u_k = \frac{2}{(n+1)^2} \frac{N\sigma_0 e^{-\alpha y} a^2 b^2}{M} \times \sum_{m=1}^n \cot^2\left(\frac{\pi}{2} \frac{m}{n+1}\right) \frac{\cos[\omega t - (\omega/V)y - \psi_m]}{\{(\omega_m^2 - \omega^2)^2 + [(B/M)\omega]^2\}^{1/2}}, \quad (\text{A6})$$

where $N = \Lambda/d_0$ (total number of movable kinks) is used. From these quantities one obtains

$$\alpha = \frac{1}{2V} \frac{Na^2 b^2 \mu}{M} \frac{2}{(n+1)^2} \sum_{m=1}^n \cot^2\left(\frac{\pi}{2} \frac{m}{n+1}\right) \times \frac{(B/M)\omega^2}{(\omega_m^2 - \omega^2)^2 + [(B/M)\omega]^2}, \quad (\text{A7})$$

$$\frac{\Delta V}{V} = \frac{1}{2} \left(\frac{Na^2 b^2 \mu}{M} \right) \frac{2}{(n+1)^2} \sum_{m=1}^n \cot^2\left(\frac{\pi}{2} \frac{m}{n+1}\right) \times \frac{\omega_m^2 - \omega^2}{(\omega_m^2 - \omega^2)^2 + [(B/M)\omega]^2}. \quad (\text{A8})$$

The contribution of the higher-order terms to α (terms $m=2$ and higher) of this expression depends on the relative magnitude of ω_m^2 against ω^2 or $(B/M)\omega$. For the worst case, i. e., ω_m^2 is much smaller than the other two, the ratio of the second term to the first is approximately $\frac{1}{4}$ for $n=9$. The larger the number of kinks in l the smaller is this ratio. In the other extreme case, i. e., ω_m^2 dominates in the denominator, the ratio becomes ap-

proximately $\frac{1}{4}$ for $n=9$. In the following we neglect the terms higher than the second:

$$u_k = \left(\frac{2}{n+1} \right) \cot\left(\frac{\pi}{2} \frac{1}{n+1}\right) \frac{\sigma_0 e^{-\alpha y} ab}{M} \sin\left(\frac{\pi k}{n+1}\right) \times \frac{\cos[\omega t - (\omega/V)y - \psi]}{\{(\omega_1^2 - \omega^2)^2 + [(B/M)\omega]^2\}^{1/2}} \\ \equiv u_{k0} \cos[\omega t - (\omega/V)y - \psi], \quad (\text{A9}) \\ \tan\psi = \frac{(B/M)\omega}{\omega_1^2 - \omega^2}, \quad \omega_1^2 = \frac{4c}{M} \sin^2\left(\frac{\pi}{2} \frac{1}{n+1}\right),$$

and

$$\alpha = \frac{1}{2V} \frac{Na^2 b^2 \mu}{M} \frac{2}{(n+1)^2} \cot^2\left(\frac{\pi}{2} \frac{1}{n+1}\right) \times \frac{(B/M)\omega^2}{(\omega_1^2 - \omega^2)^2 + [(B/M)\omega]^2}, \quad (\text{A10})$$

$$\frac{\Delta V}{V} = \frac{1}{2} \frac{Na^2 b^2 \mu}{M} \frac{2}{(n+1)^2} \cot^2\left(\frac{\pi}{2} \frac{1}{n+1}\right) \times \frac{\omega_1^2 - \omega^2}{(\omega_1^2 - \omega^2)^2 + [(B/M)\omega]^2}. \quad (\text{A11})$$

In the limiting case of $d_0/l \ll 1$ (or n large), these expressions agree exactly with those obtained by Suzuki and Elbaum.³⁴ In the other extreme case of $d_0/l = \frac{1}{2}$ (or $n=1$), the latter overestimates α by a factor of $4/\pi$.

*Research supported in part by the Office of Naval Research, by the National Science Foundation, and by the Advanced Research Projects Agency.

¹W. G. Johnston and J. J. Gilman, *J. Appl. Phys.* **30**, 129 (1959).

²For conduction electrons, V. Ya. Kravchenko, *Fiz. Tverd. Tela* **8**, 927 (1966) [*Sov. Phys.-Solid State* **8**, 740 (1966)]; calculation due to T. Holstein, quoted by B. R. Tittman and H. E. Bömmel, *Phys. Rev.* **151**, 178 (1966); A. D. Brailsford, *ibid.* **186**, 959 (1969).

³For phonons, A. D. Brailsford, *J. Appl. Phys.* **43**, 1380 (1972), and the references therein.

⁴V. I. Alshits, *Zh. Eksp. Teor. Fiz.* **63**, 1829 (1972) [*Sov. Phys.-JETP* **36**, 978 (1973)].

⁵A. Hikata and C. Elbaum, *Phys. Rev. Lett.* **18**, 750 (1967); A. Hikata and C. Elbaum, *Trans. Jap. Inst. Metals Suppl.* **9**, 46 (1968); R. A. Johnson, thesis (Brown University, 1971) (unpublished).

⁶A. Hikata, R. A. Johnson, and C. Elbaum, *Phys. Rev. B* **2**, 4856 (1970); **4**, 674(E) (1971).

⁷A. Hikata, J. Deputat, and C. Elbaum, *Phys. Rev. B* **6**, 4008 (1972).

⁸R. J. Blume, *Rev. Sci. Instrum.* **34**, 1400 (1963).

⁹B. B. Chick (unpublished).

¹⁰K. Lücke and J. Schlipf, *Proceedings of the Symposium on the Interaction between Dislocations and Point Defects*, Harwell, 1968, Atomic Energy Research Establishment, AERE-R5944, p. 118 (unpublished).

¹¹H. M. Simpson and A. Sosin, *Phys. Rev. B* **5**, 1382 (1972).

¹²L. M. Brown, *Phys. Status Solidi* **1**, 585 (1961).

¹³J. L. Tallon and W. H. Robinson, *Philos. Mag.* **27**,

985 (1973).

¹⁴T. Kurosawa, *J. Phys. Soc. Jap.* **19**, 2096 (1964).

¹⁵A. Seeger, *Philos. Mag.* **1**, 651 (1956).

¹⁶J. Friedel, *Dislocations* (Pergamon, New York, 1964), p. 72.

¹⁷G. Schottky, *Phys. Status Solidi* **5**, 697 (1964).

¹⁸W. T. Sanders, *J. Appl. Phys.* **36**, 2822 (1965).

¹⁹A. C. Anderson and M. E. Malinowski, *Phys. Rev. B* **5**, 3199 (1972).

²⁰G. Alefeld, *J. Appl. Phys.* **36**, 2633 (1965); **36**, 2642 (1965).

²¹F. Kroupa and L. M. Brown, *Philos. Mag.* **6**, 1267 (1961).

²²A. D. Brailsford, *Phys. Rev.* **122**, 778 (1961); **128**, 1033 (1962).

²³A. Seeger and P. Schiller, *Acta Met.* **10**, 348 (1962).

²⁴W. P. Mason, *Fundamental Aspects of Dislocation Theory*, Natl. Bur. Stand. Spec. Publ. No. 317 (U. S. GPO, Washington, D. C., 1970), Vol. 1, p. 447.

²⁵T. Suzuki and C. Elbaum, *J. Appl. Phys.* **35**, 1539 (1964).

²⁶A. Granato and K. Lücke, *J. Appl. Phys.* **27**, 583 (1956).

²⁷J. D. Eshelby, *Proc. R. Soc. A* **226**, 222 (1962).

²⁸E. W. Hart, *Phys. Rev.* **98**, 1775 (1955).

²⁹F. R. N. Nabarro, *Theory of Crystal Dislocations* (Oxford U. P., Oxford, England, 1967), p. 505.

³⁰V. I. Alshits, V. L. Indenbom, and A. A. Shtolberg, *Phys. Status Solidi* **B50**, 59 (1972).

³¹H. Suzuki, *Introduction to Dislocation Theory* (in Japanese) (AGNE Publishing Co., Tokyo, 1967), p. 272.

³²J. H. Weiner, *Phys. Rev.* **136**, A863 (1964).

- ³³L. S. Jacobsen, *Trans. Am. Soc. Mech. Eng.* 52 (1), 169 (1930).
- ³⁴G. Alefeld, J. Filloux, and H. Harper, *Dislocation Dynamics*, edited by R. Rosenfield, G. T. Hahn, A. Bement, Jr., and R. I. Jaffe (McGraw-Hill, New York, 1968), p. 191.
- ³⁵W. P. Mason, *J. Geophys. Res.* 74, 4963 (1969).
- ³⁶W. P. Mason and J. Wehr, *J. Phys. Chem. Solids* 31, 1925 (1970).
- ³⁷W. P. Mason, in Ref. 34, p. 487.
- ³⁸T. Suzuki, A. Ikushima, and M. Aoki, *Acta Met.* 12, 1231 (1964).
- ³⁹A. Seeger and H. Engelke, in Ref. 34, p. 623; see also Agenda discussion, p. 609.
- ⁴⁰A. Ookawa and K. Yazu, *J. Phys. Soc. Jap. Suppl.* 18, 36 (1963).
- ⁴¹R. den Buurman and D. Weiner, *Scripta Met.* 5, 573 (1971).
- ⁴²K. Lücke and G. Roth, *Scripta Met.* 5, 757 (1971).
- ⁴³V. K. Paré and H. D. Guberman, *J. Appl. Phys.* 44, 32 (1973).
- ⁴⁴D. O. Thompson and O. Buck, *Phys. Status Solidi* 37, 53 (1970).
- ⁴⁵G. Roth, G. Sokolowski, and K. Lücke, *Phys. Status Solidi* 40, K77 (1970).